

# Exploring Deep Models for Practical Gait Recognition

Chao Fan<sup>1,2</sup>, Saihui Hou<sup>3,4</sup>, Yongzhen Huang<sup>3,4</sup>, Shiqi Yu<sup>1,2\*</sup>

<sup>1</sup> Department of Computer Science and Engineering, Southern University of Science and Technology

<sup>2</sup> Research Institute of Trustworthy Autonomous System, Southern University of Science and Technology

<sup>3</sup> School of Artificial Intelligence, Beijing Normal University <sup>4</sup> WATRIX.AI

{12131100}@mail.sustech.edu.cn, {housaihui, huangyongzhen}@bnu.edu.cn, yusq@sustech.edu.cn

## Abstract

Gait recognition is a rapidly advancing vision technique for person identification from a distance. Prior studies predominantly employed relatively small and shallow neural networks to extract subtle gait features, achieving impressive successes in indoor settings. Nevertheless, experiments revealed that these existing methods mostly produce unsatisfactory results when applied to newly released in-the-wild gait datasets. This paper presents a unified perspective to explore how to construct deep models for state-of-the-art outdoor gait recognition, including the classical CNN-based and emerging Transformer-based architectures. Consequently, we emphasize the importance of suitable network capacity, explicit temporal modeling, and deep transformer structure for discriminative gait representation learning. Our proposed CNN-based DeepGaitV2 series and Transformer-based SwinGait series exhibit significant performance gains in outdoor scenarios, e.g., about +30% rank-1 accuracy compared with many state-of-the-art methods on the challenging GREW dataset. This work is expected to further boost the research and application of gait recognition. Code will be available at <https://github.com/ShiqiYu/OpenGait>.

## 1. Introduction

Gait is a biometric characteristic that presents the unique walking patterns of individuals. Compared with other biometric modalities, e.g., face, fingerprint, and iris, gait is hard to disguise and can be easily captured at a distance in non-intrusive ways without requiring cooperation. For these advantages, gait recognition is one of the most feasible techniques for security applications, such as suspect tracking, crime prevention, and identity verification [33].

The widely-verified effectiveness and robustness of deep architectures [36, 27, 40, 1] greatly promote various vision techniques. Gait recognition utilizing deep models has also achieved a series of impressive successes [42, 4]. How-

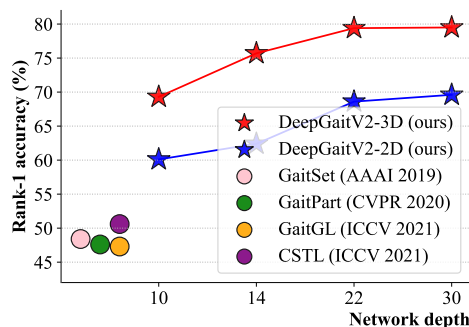


Figure 1. Rank-1 accuracy on the challenging GREW [46].

ever, existing methods mainly use relatively small, shallow neural nets, instead of really deep ones, and little attention has been given to the underlying reasons. We believe that the leading cause may be the prevalent input modality for gait recognition, i.e., the binary silhouette, which is structurally simple and characteristically sparse, thereby being considered not to require a very deep and large model. Nowadays, gait recognition has rapidly matured, shifting from constrained testing in the lab [44, 38] to real applications in the wild [46, 45]. Nevertheless, unprecedented challenges, such as complex backgrounds, severe occlusion, unpredictable illumination, arbitrary viewpoints, and diverse clothing changes, have significantly reduced the performance of most representative methods on outdoor gait datasets [46, 8]. To make deep gait models robust and strong, this paper provides several empirical principles to cope with the vast complexities of outdoor gait recognition.

In principle, deep architectures can learn features at various levels of abstraction, and reasonable network depth largely determines the model’s capacity to dispel noisy factors. Thus, to address the complicated challenges that arise with newly proposed outdoor gait datasets, we naturally increase the depth of the proposed DeepGaitV2 <sup>1</sup>. The results

<sup>1</sup>We regard GaitBase in [8] as a pioneering attempt to explore deep ResNet [13] for gait modeling and call it DeepGaitV1. Hence, the network architectures proposed in this work are named DeepGaitV2.

\*Corresponding Author

demonstrate that *the accuracy improves with the reasonably increased depth and finally reaches a breakthrough on the challenging outdoor GREW [46], i.e., about +30% rank-1 accuracy improvement* as shown in Figure 1. However, the nearly reverse results can be obtained on two other indoor gait datasets, *i.e.*, CASIA-B [44] and OU-MVLP [38]. After conducting a comprehensive experiment and in-depth analysis, we emphasize the importance of suitable network capacity in extracting the features of characteristically sparse silhouette data.

Another crucial aspect of gait recognition is learning the temporal changes that present walking patterns of individuals, especially when the appearance features are relatively unreliable (*e.g.*, bag-carrying, cloth-changing, and partial occlusion). Currently, two methodologies prevail in the gait research community, *i.e.*, regarding the gait as a set [4] or sequence. These two kinds of works have performed similar achievements in the past few years by using relatively shallow nets. Among them, the set-based methods attract relatively more attention [20, 11] thanks to their advantages of flexible input and concise architecture. However, this paper shows that *the sequence-based DeepGaitV2 significantly outperforms its set-based counterpart* on varying gait datasets. Since the plain sequence-based DeepGaitV2 contains much more training parameters, to exclude the potential positive influence, we propose a lightweight version of sequence-based DeepGaitV2, which also outperforms the set-based counterpart by a large margin with similar computational complexity. Through extensive experiments and analyses, we empirically confirm the superiority of exact characterizing dependencies between successive frames for discriminative gait representation learning.

Furthermore, witnessing a modeling shift from CNNs to Transformers [39, 6, 25], deep gait transformer presents an attractive opportunity for tackling the complexities of outdoor environments. Nevertheless, unlike the float-encoding RGB image patch, a significant portion of input patches generated by partitioning the gait silhouette is all-white or all-black, resulting in massive non-informative or even invalid gradients in computing self-attention at the bottom of the deep transformer backbone. To solve this problem, we provide a straight solution and thus build **SwinGait**. To our knowledge, SwinGait is the first transformer-based gait recognition method that surpasses prior works by a significant margin on various large-scale outdoor gait datasets [45, 46]. Also, SwinGait outperforms our DeepGaitV2 series in most cases, convincingly exhibiting the promising future of deep gait transformer in outdoor applications.

In conclusion, this paper presents a comprehensive approach to constructing deep models for gait recognition, structurally consisting of CNN-based and Transformer-based architectures and technically involving the empirical principles used to determine network capacity, develop tem-

poral model, and build gait transformer. We hope that DeepGaitV2 can promote further developments in CNN-based models, and that SwinGait can bring about a modeling shift in gait recognition.

## 2. Related Works

According to the classical taxonomy, gait recognition methods can be broadly divided into model-based and appearance-based categories. The former typically takes the estimated underlying structure of the human body, such as 2D/3D pose [2, 31] and SMPL model [28], as input, while the latter tends to extract the gait features from silhouettes directly. While model-based methods [23, 22] are theoretically robust to real-world factors, such as dressing and carrying, it is challenging to accurately estimate body posture characteristics from low-resolution videos. Therefore, appearance-based methods, which are relatively suitable for practical usage, have become the most commonly used approach in the literature. This section will discuss these methods from three perspectives: deep spatial, temporal, and transformer approaches for gait feature extraction.

**Deep Spatial Feature Extraction.** Wu *et al.* [42] were among the pioneering researchers to introduce deep neural networks into gait recognition. Thereafter, Chao *et al.* [4] adopted a part-based model for human body description, which is still widely used today. Fan *et al.* [9] suggested that the recognition models should focus on more local details and presented FConv Layer. Lin *et al.* [24] highlighted the importance of combining spatially local and global features for discriminative gait pattern description. Zheng *et al.* [45] leveraged human mesh to access 3D geometric information for enhanced posture representation. Dou *et al.* [7] devised a sophisticated attention module to facilitate the learning of spatiotemporal gait features. These works typically employ stacked layers with a maximum depth of ten to capture the subtle identity characteristics against massive complexities in real-world scenes, such as varying viewpoints, dress changes, bag carrying, and intractable occlusion. Despite achieving notable success in the classical indoor gait datasets, *i.e.*, CASIA-B [44] and OU-MVLP [38], these representative methods often suffer from a significant performance degradation on the challenging outdoor gait datasets [8]. This phenomenon stimulates the necessity to rethink deep gait models' design principles for applications.

**Deep Temporal Modeling** is always one of the most attractive topics for gait recognition because of the specification of walking movement, *i.e.*, periodicity. Two popular methodologies exist in the literature: set-based [4] and sequence-based [41] viewpoints. The former believes the order information of the gait video is not necessary for presenting the unique individual characteristics since people can roughly identify the position of each frame in the gait cycle according to the appearance. Practically, the set-based methods [4, 15, 16] extract silhouette fea-

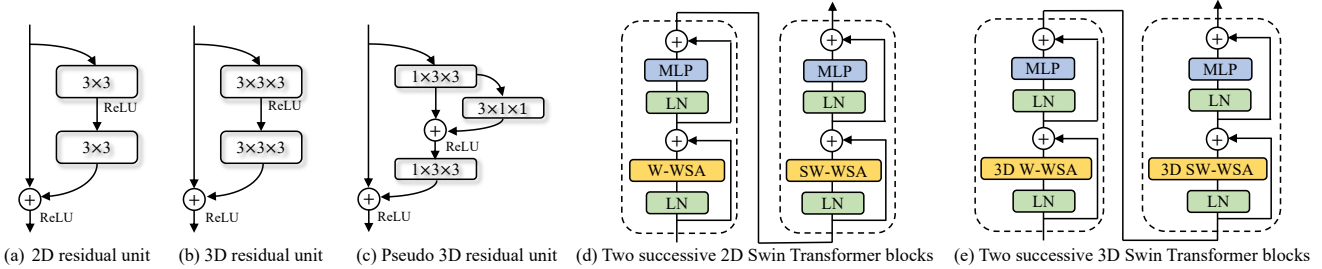


Figure 2. Employed basic blocks, including the convolution-based (a) 2D, (b) 3D and (c) Pseudo 3D residual blocks [13, 12, 35], the transformer-based (d) 2D and (e) 3D Swin Transformer blocks [25, 26].

tures frame by frame and then learn a sequence-level feature using a max-pooling function along the temporal dimension. Although the sequence-based methods that explicitly capture features from consecutive frames generally achieve slightly better performance, the set-based methods are preferred due to their superior efficiency and robustness to noise [46, 45, 20, 11]. Nonetheless, in the future part of this paper, we emphasize the superiority of sequence-based methodology for gait representation learning.

**Deep Gait Transformer.** Several works attempt to introduce the deep transformer into gait recognition, *e.g.*, Mogan *et al.* [32], and Pinvcic *et al.* [34] directly employ the prevailing ViT model [6] on gait silhouette, and Cui *et al.* [5] use sequence transformer for gait temporal modeling. Currently, the transformer-based methods did not achieve impressive results on the popular testing benchmarks, especially for the challenging in-the-wild gait datasets [46, 45]. But we still believe the transformer structure can achieve promising results as they work on other vision topics.

### 3. Deep Models for Practical Gait Recognition

The aim of this paper is to explore deep models for gait recognition from a high-level systematic perspective. This section will reveal that suitable network capacity, explicit temporal modeling, and deep vision transformers can effectively benefit gait representation learning. To this end, we introduce multiple essential layers that will be used to form the deep gait models. Then, we revisit the general gait recognition framework and specifically instantiate it with plenty of architectural variants, proposing the powerful convolution-based DeepGaitV2 and transformer-based SwinGait series. Following a comprehensive experimental study and analysis, we summarize the crucial empirical principles for deep gait recognition research.

#### 3.1. Employed Blocks

As shown in Figure 2, various fundamental building blocks are deployed to make up our deep gait models. Among them, the 2D residual unit is a popular structure for constructing very deep models [13]. Figure 2 (b) presents its 3D counterpart. Figure 2 (c) shows the pseudo 3D residual

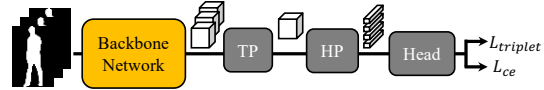


Figure 3. Overall architecture. The TP and HP respectively denote Temporal and Horizontal Pooling. The Head comprises the separate fully-connected and BNNeck [30] layers.

unit composed of a 1D temporal and two 2D spatial convolution layers. The recently popular vision transformer layer, *i.e.*, Swin Transformer [25] and its 3D variant [26] shown in Figure 2 (d) and (e), are also incorporated to create powerful transformer-based gait models.

In this paper, the primary goal is not to modify these general-purpose blocks, as their universal effectiveness has been validated across many vision tasks. Our main novelty lies in leveraging these powerful basic blocks to learn fine-grained gait features from a systematic perspective.

#### 3.2. Revisit Gait Recognition Pipeline

Figure 3 presents a common gait recognition framework, and the framework is widely accepted by the research community as summarized in [8]. To keep this overview brief, we will only focus on the overall pipeline and omit the specific structures of particular layers and blocks.

As illustrated in Figure 3, the gait sequence with  $T$  silhouette images is first fed through the backbone, and a sequence of 3D feature maps with the height, width, and channel dimensions can be generated. Then, the widely-utilized Temporal Pooling (TP) operation [4, 9, 24] is employed to facilitate sequence aggregation, which is usually instantiated as a simple maximum function along the temporal dimension. Thereafter, the obtained feature map is horizontally divided into several parts, which are further pooled into feature vectors through the popular Horizontal Pooling (HP) operation [10]. Besides, the popular part-based paradigm [37] is adopted as the feature mapping strategy. The separated fully connected layers are used to map the feature vectors, and the prevailing BNNeck [30] is leveraged to adjust the metric space. Lastly, the separate triplet and cross-entropy losses are employed to form the overall loss function formulated by  $L = L_{triplet} + L_{ce}$ .

Table 1. Architecture for convolution-based DeepGaitV2 including both the 2D and 3D versions. Employed blocks are shown in brackets (see also Figure 2 (a) and (b)), with the numbers of blocks stacked. Down-sampling is performed by Layer2 and Layer3 with a stride of 2.  $T$  and  $C$  respectively denote the input sequence length and arbitrary channel number.

Layers	Output feature map size	DeepGaitV2-2D				DeepGaitV2-3D					
		Block structure	10-layer	14-layer	22-layer	30-layer	Block structure	10-layer	14-layer	22-layer	30-layer
Conv0	$(T, C, 64, 44)$	$3 \times 3$ , stride 1									
Stage1	$(T, C, 64, 44)$	$\begin{bmatrix} 3 \times 3, C \\ 3 \times 3, C \end{bmatrix}$	$\times 1$	$\times 1$	$\times 1$	$\times 1$	$\begin{bmatrix} 3 \times 3, C \\ 3 \times 3, C \end{bmatrix}$	$\times 1$	$\times 1$	$\times 1$	$\times 1$
Stage2	$(T, 2C, 32, 22)$	$\begin{bmatrix} 3 \times 3, 2C \\ 3 \times 3, 2C \end{bmatrix}$	$\times 1$	$\times 2$	$\times 4$	$\times 4$	$\begin{bmatrix} 3 \times 3 \times 3, 2C \\ 3 \times 3 \times 3, 2C \end{bmatrix}$	$\times 1$	$\times 2$	$\times 4$	$\times 4$
Stage3	$(T, 4C, 16, 11)$	$\begin{bmatrix} 3 \times 3, 4C \\ 3 \times 3, 4C \end{bmatrix}$	$\times 1$	$\times 2$	$\times 4$	$\times 8$	$\begin{bmatrix} 3 \times 3 \times 3, 4C \\ 3 \times 3 \times 3, 4C \end{bmatrix}$	$\times 1$	$\times 2$	$\times 4$	$\times 8$
Stage4	$(T, 8C, 16, 11)$	$\begin{bmatrix} 3 \times 3, 8C \\ 3 \times 3, 8C \end{bmatrix}$	$\times 1$	$\times 1$	$\times 1$	$\times 1$	$\begin{bmatrix} 3 \times 3 \times 3, 8C \\ 3 \times 3 \times 3, 8C \end{bmatrix}$	$\times 1$	$\times 1$	$\times 1$	$\times 1$
TP	$(1, 8C, 16, 11)$	Temporal Pooling									
HP	$(1, 8C, 16, 1)$	Horizontal Pooling									
Head	$(1, 8C, 16, 1)$	Flatten, 16 separate fully-connected layers and BNNecks [30]									

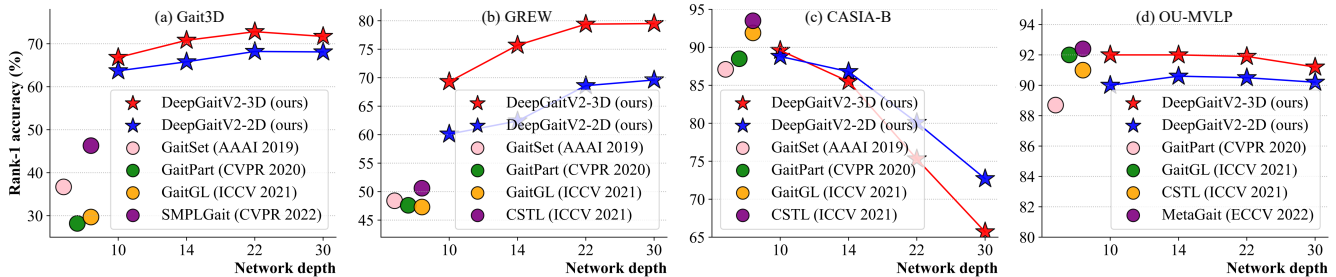


Figure 4. Rank-1 accuracy of DeepGaitV2-2D/3D with backbone network going deeper on Gait3D [45], GREW [46], CASIA-B [44] and OU-MVLP [38]. The performance of several state-of-the-art methods are introduced for reference, such as GaitSet [4], GaitPart [9], GaitGL [24], CSTL [19], SMPLGait [45], and MetaGait [7]. Note the accuracy on CASIA-B is the average of three testing subsets.

### 3.3. Superiority of Suitable Network Capacity

Beginning with AlexNet [21], the remarkable architectural advances of backbone networks, *e.g.*, the increased depth [13] and more extensive connections [17], have enhanced numerous vision tasks with impressive achievements. Yet, prior gait recognition methods typically employ relatively small and shallow neural networks. The superiority of very deep backbones remains to be established. We conduct a comprehensive study to explore the effectiveness of very deep models in learning gait representation.

**Proposed DeepGaitV2.** As shown in Tab. 1, the backbones of DeepGaitV2 series, including DeepGaitV2-2D and its 3D counterpart, are all composed of five basic layers, *i.e.*, the initial convolution layer (Conv0) and the following residual layers (Stage 1 to 4). The number of residual blocks stacked on each stage (denoted as  $B$ ) directly determines the network depth. For example, if the  $B$  is set to [1,1,1,1], the network depth would be  $2 \times (1+1+1+1)+2=10$ , where the last +2 implies the initial Conv0 and the final head layers. Therefore, as shown in Tab. 1, we obtain a serial of DeepGaitV2-2D/3D with 10 layers, 14 layers, 22 layers and 30 layers. Note that Stage 1 of DeepGaitV2-3D is still formed by 2D residual blocks for computational efficiency.

**Success on Nowadays Outdoor Datasets.** As shown in Figure 4 (a) and (b), the DeepGaitV2 series significantly outperform prior state-of-the-art methods, *i.e.*, +20% ~ 30% rank-1 accuracy on Gait3D [45] and GREW [46], two of the most large-scale outdoor gait datasets. Additionally, there is a little performance degradation and an early performance saturation at a depth of 30 layers on Gait3D and GREW, respectively. This experimentally indicates that, for outdoor gait datasets like Gait3D and GREW, the appearance-based gait models need a suitable network depth, either not too shallow (less than 10 layers like prior methods typically employed) or very deep (more than 30 layers like many RGB-based vision tasks widely used).

**Unsatisfied Performance on Indoor Datasets.** As shown in Figure 4 (c) and (d), it can be observed that on CASIA-B [44], the performance of DeepGaitV2 dramatically drops with the increasing network depth, quickly becoming incomparable to other state-of-the-art methods. On the other hand, when evaluating on OU-MVLP [38], the DeepGaitV2 series remain competitive throughout. However, it still shows a slight performance decrease after a 22-layer depth.

Though CASIA-B and OU-MVLP are two of the most widely-employed gait datasets in the latest literature, they

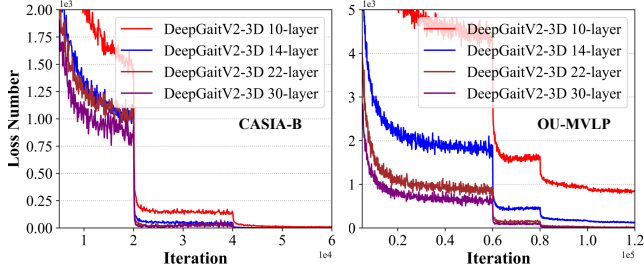


Figure 5. DeepGaitV2-3D series meet the over-fitting cases with the increasing network depth on CASIA-B [44] and OU-MVLP [38]. The loss number presents the count of triplets that cause non-zero loss in a training batch, directly reflecting the network’s convergence state.

are both captured in totally-constrained laboratory environments, which limits the diversity of samples for training. The former has only 74 subjects for training, and the latter includes just view-changing factors. The two datasets are far from a simulation of the real-world, such as long-term cloth-changing, serious occlusion, unpredictable illumination, and arbitrary viewpoints. Since deep model training requires a large volume of diverse samples to achieve a good performance, there should be an over-fitting in implementing the DeepGaitV2 series on these two indoor gait datasets. Further experiments shown in Figure 5 confirm the assumption. The 30-layer DeepGaitV2-3D converges obviously faster but performs worse than its 10-layer counterpart on both datasets.

**Empirical Principle #1.** We consider that the deep gait models should possess a suitable capacity. Based on the empirical results shown in Figure 4, a depth of 10-layer and 22-layer is respectively satisfactory for the current indoor and outdoor gait datasets. Unless otherwise stated, the 10-layer and 22-layer DeepGaitV2 are chosen as the standard models for indoor and outdoor implementations.

### 3.4. Superiority of Explicit Temporal Modeling

The gait pattern typically combines static appearance characteristics and dynamic movement features. Therefore, capturing the changes that occur over time in the walking process is critical in discriminative gait representation learning. Recently, regarding gait as a set of unordered silhouettes [4] has become increasingly popular [43, 20, 11, 16]. Its core idea comes from the observation that people can easily identify a certain temporal position of a silhouette in the gait cycle merely by looking at its appearance since the walking process is usually periodic. Therefore, the set-based methods consider order information unnecessary and tend not to explicitly make use of the motion features among neighboring frames. Instead, they utilize a single maximum operation along the temporal dimension to aggregate the global features of a gait sequence.

However, our experiments show the sequence-based

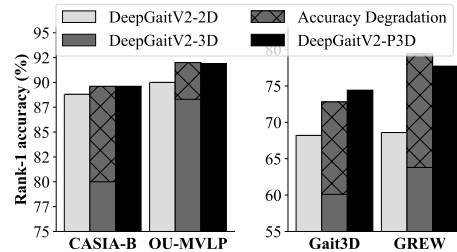


Figure 6. Rank-1 accuracy of DeepGaitV2-2D/3D/P3D on CASIA-B [44], OU-MVLP [38], Gait3D [45] and GREW [46]. The shaded area presents the accuracy degradation of DeepGaitV2-3D when the input video is shuffled.

DeepGaitV2 clearly surpasses its set-based counterpart on various mainstream gait datasets, *i.e.*, CASIA-B [44], OU-MVLP [38], Gait3D [45] and GREW [46]. Notably, DeepGaitV2-2D and its 3D counterpart respectively present the plain set-based and sequence-based DeepGaitV2 since the former only consists of 2D residual blocks, and the latter mainly consists of 3D blocks, as shown in Tab. 1.

As depicted in Figure 6, DeepGaitV2-3D surpasses its 2D counterpart by +0.8%, +2.0%, +4.6%, +10.8% on CASIA-B [44], OU-MVLP [38], Gait3D [45] and GREW [46], respectively. Additionally, when the input sequence is shuffled to explore the role of dependencies between neighboring silhouettes (destroying the sequential characteristics), there is a noticeable accuracy degradation as shown by the shaded area in Figure 6, *i.e.*, -9.6%, -3.7%, -12.7%, -15.8% on CASIA-B, OU-MVLP, Gait3D, and GREW, respectively. The results convincingly highlight the benefit of explicit temporal modeling for gait.

Moreover, since DeepGaitV2-3D has significantly more training parameters than its 2D counterpart, some may argue that the performance gain is simply brought by the additional parameters and computational cost (27.5 *v.s.* 9.3 MB and 6.8 *v.s.* 2.4 GFLOPs per silhouette image)<sup>2</sup>. To address the concern, we develop a lightweight yet powerful sequence-based DeepGaitV2, *i.e.*, DeepGaitV2-P3D.

**Proposed DeepGaitV2-P3D.** DeepGaitV2-P3D is designed based on DeepGaitV2-3D by replacing all its 3D residual blocks with their corresponding pseudo 3D blocks. Figure 2 (c) [35] illustrates the employed pseudo 3D residual block, which merely requires one additional 1D temporal convolution in comparison to its 2D counterpart shown in Figure 2 (a) [13]. This translates to only a minor increase in training parameters (11.1 *v.s.* 9.3 MB) and computational cost (2.9 *v.s.* 2.4 GFlops per silhouette image).

As shown in Figure 6, DeepGaitV2-P3D achieves the totally competitive or even superior performance than its 3D counterpart (-0.04%, -0.1%, +1.6%, -1.7% on CASIA-B, OU-MVLP, Gait3D and GREW, respectively.). Furthermore, DeepGaitV2-P3D is superior to its 2D counterpart

<sup>2</sup>Here we only consider the backbone. The same below.

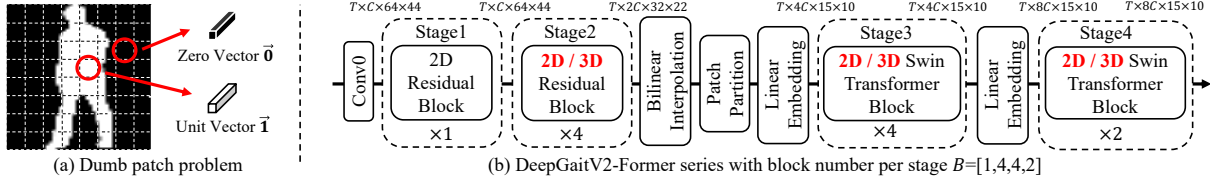


Figure 7. (a) Directly partitioning silhouette results in lots of dumb patches. (b) Overall architecture of SwinGait-2D/3D.

over all the testing datasets, *i.e.*, +0.8%, +1.9%, +6.2%, +9.1% on CASIA-B, OU-MVLP, Gait3D and GREW, respectively. This experiment shows the superiority of explicitly capturing motion details, even when the sequence-based DeepGaitV2 has a similar model size and computation cost compared with its set-based counterpart.

**Empirical Principle #2.** The order of frames in a sequence can be regarded as the inherent time stamps, precisely guiding the fusion of locally adjacent frames for a fine-grained extraction of motion features. We suggest adequately using the sequential priors instead of ignoring them completely. DeepGaitV2-3D and its P3D counterpart are two of the most direct instances for deep gait temporal modeling.

### 3.5. Superiority of Deep Gait Transformer

Though CNN-based architectures still remain dominant in gait recognition, the transformer-based models have reached a series of state-of-the-art achievements in many computer vision tasks, *e.g.*, image recognition [25, 6] and action recognition [26]. Recently, an innovative self-attention mechanism with shifted window [25] has successfully enhanced the vision temporal cues description [26], thus inspiring us to explore the advanced transformer-based model for spatiotemporal gait representation learning.

**Proposed SwinGait.** Technically, transformer-based models usually split an input RGB image into non-overlapping patches. Each patch is treated as a ‘token’, and its feature is set as a concatenation of the raw pixel of RGB values. Then, the self-attention mechanism or its variant is performed on the linear embedding of these tokens.

However, as shown in Figure 7 (a), many patches on a gait silhouette are all-white (all 1.0) or all-black (all 0.0). These patches provide neither posture nor shape information of the human body. Therefore, we call them dumb patches. Further statistics present that 84.1% patches are dumb in GREW [46] when the image size is  $64 \times 64$  and the patch size is  $4 \times 4$ . Since all values from a dumb patch are all 0 or all 1, dumb patches can make backward gradients characteristically useless or even computationally invalid in optimizing the training parameters of the bottom transformer layers. A naive solution is to use a larger patch size, *e.g.*, setting patch size to  $16 \times 16$  results in only 46.2% dumb patches in GREW [46]. Nevertheless, this means the silhouette will be directly down-sampled by 1/16 at the input layer, *i.e.*, only  $\frac{64}{16} \times \frac{64}{16} = 16$  tokens will be fed into the

following transformer backbone. It is difficult to hierarchically capture the subtle spatiotemporal gait changes.

We adopt another straightforward coping strategy shown in Figure 7 (b), *i.e.*, instantiating the first two stages as convolution blocks. Thanks to the sliding window mechanism and nonlinear modeling capability of the convolution layers, Conv0, Stage 1 and Stage 2 can transform the binary silhouette data to the float-encoding feature map to provide dense and abundant low-level structural features, such as edge and shape information. The following transformer layers, *i.e.*, Stage 3 and Stage 4, will then leverage the advanced transformer-based modules to learn the high-level identification features. We employ the widely-accepted 2D and 3D Swin Transformer blocks [25, 26] shown in Figure 2 (d) and (e) to construct SwinGait-2D and its 3D counterpart, respectively. The main reasons are two-fold: a) Performing self-attention in the local spatiotemporal window enables the exploration of local appearance and motion details for fine-grained gait description. b) The excellent speed-accuracy trade-off of Swin Transformer attracts us a lot.

As shown in Figure 7 (b), the exact structures of Conv0, Stage 1 and Stage 2 in SwinGait-2D/3D are totally the same as that in the proposed DeepGaitV2-2D/3D for fair comparisons<sup>3</sup>. After these convolution blocks, the feature maps are with size of  $T \times 2C \times 32 \times 22$  tensor, where  $T$  is the number of frames, and  $C$  is the number of channels. To match the size limit required by the downstream transformer blocks, these feature maps are resized to  $2C \times 30 \times 20$  frame by frame via a bilinear interpolation layer. Then, we treat each 3D patch of size  $2C \times 2 \times 2$  as a token. Thus, the 3D patch partitioning layer obtains  $T \times \frac{30}{2} \times \frac{20}{2}$  3D tokens, with each patch/token consisting of a  $8C$ -dimensional feature. A linear embedding layer is then applied to project the feature of each token to a  $4C$ -dimensional vector.

Stage 3 and 4 in SwinGait-2D/3D are composed of the standard 2D/3D Swin Transformer block proposed by Liu *et al* [25, 26]. Specifically, the 2D Swin Transformer [25] is built by replacing the standard multi-head self-attention module in a Transformer [39] block with a module based on shifted windows. As shown in Figure 8 (a), the 2D shifted windows bridge the windows of the preceding layer, providing connections among them (inducing bias for spatial locality). Since there are no connections along the temporal

<sup>3</sup>On Gait3D [45], SwinGait-3D inherits DeepGaitV2-P3D since the latter performs better than its 3D counterpart.

Table 2. Implementation details. #LR and #WD present the initial learning rate and weight decay.  $T$  and  $C$  respectively denote the input sequence length and arbitrary channel number shown in Tab. 1 and Figure 7. The batch size  $(q, k)$  indicates  $q$  subjects with  $k$  sequences per subject. The  $I_{max}$  presents the maximum number of iterations per half-cosine period.

Datasets	Batch size	DeepGaitV2 series, $T=30, C=64$				SwinGait series, $T=30, C=64$			
		Optimizer	Scheduler			Optimizer	Scheduler		
			Type	Milestones	Total steps		Type	$I_{max}$	Total steps
CASIA-B [44]	(8,16)	SGD #LR= $1 \times 10^{-1}$ #WD= $5 \times 10^{-5}$	Multi-step (drop by 1/10 per milestone)	[20k, 40k, 50k]	60k	AdamW [29]	Cosine-	-	
OU-MVLP [38]	(32,8)			[60k, 80k, 100k]	120k	#LR= $3 \times 10^{-4}$	annealing	-	
Gait3D [45]	(32, 4)			[20k, 40k, 50k]	60k	#WD= $2 \times 10^{-2}$	(update per	60k	80k
GREW [46]	(32, 4)			[80k, 120k, 150k]	180k	#LR $_{min}$ = $3 \times 10^{-5}$	1k steps)	150k	200k

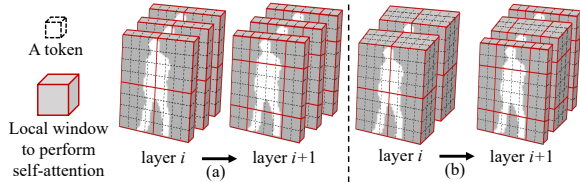


Figure 8. An illustrated example of (a) 2D and (b) 3D shifted window [25, 26]. In this case, the window size is set to (a) (1, 4, 4) and (b) (3, 4, 4) with temporal, height, and width dimensions.

dimension in the 2D Swin Transformer, the 3D Swin Transformer serves as a spatiotemporal adaptation of its 2D counterpart. As shown in Figure 8 (b), the 3D Swin Transformer extends the scope of local attention computation from only the spatial domain to the spatiotemporal domain, thereby inducing bias for the spatiotemporal locality.

In our implementation, the 3D window size of 2D and 3D Swin Transformer block is set to (1, 3, 5) and (3, 3, 5). Moreover, Stage 3 and Stage 4 are connected by another linear embedding layer responsible for mapping the feature of each token to a  $8C$ -dimensional vector.

**Empirical Principle #3.** The dumb patch problem and spatiotemporal locality exploration are considered two of the most fundamental challenges for developing the deep gait transformer. Among them, the former directly impacts the optimization process, and the latter primarily influences the fine-grained description of subtle gait characteristics. The experiments demonstrate that our SwinGait can solve the challenges effectively. We hope the SwinGait series can further advance the modeling shift, *i.e.*, from CNN-based to Transformer-based, in deep gait representation learning.

## 4. Experiments

For a convincing elaboration, some experiments have been briefly described in the previous section along with exploring deep models for gait recognition. In this section, we will first provide the details of datasets and implementation for completeness, and then we will perform the comparison with state-of-the-art methods and the ablation study.

### 4.1. Setup

**Datasets.** Four widely-used gait datasets are employed, *i.e.*, CASIA-B [44], OU-MVLP [38], Gait3D [45], and

Table 3. Datasets in use. #ID and #Seq present the number of identities and sequences.

DataSet	Train Set		Test Set		Collection situations
	Id	Seq	Id	Seq	
CASIA-B [44]	74	8,140	50	5,500	In-the-lab
OU-MVLP [38]	5,153	144,284	5,154	144,412	In-the-lab
Gait3D [45]	3,000	18,940	1,000	6,369	In-the-wild
GREW [46]	20,000	102,887	6,000	24,000	In-the-wild

GREW [46]. They were collected in 2006, 2018, 2022, and 2021, respectively, with the collection scenes of the former two being fully-constrained laboratories and those of the latter two being entirely in the wild. The key statistical indicators are shown in Tab. 3. Our experiments strictly follow the official evaluation protocols.

**Implementation Details.** Most of the implementation details are presented in Table 2. Unless otherwise specified, a) the silhouettes are aligned by the normalization method used in [38] and resized to  $64 \times 44$ . b) The input sequence is unordered for implementing the DeepGaitV2-2D and SwinGait-2D while ordered for others. c) The triplet loss with a margin of 0.2 is used [14]. d) The spatial augmentation strategy outlined by [8] is adopted. e) The source code will be available. Particularly for the SwinGait series, a) The bottom convolution and head layers are initialized from the corresponding trained DeepGaitV2 model [3] with the learning rate of  $3 \times 10^{-5}$ . b) Following [25], a stochastic depth rate of 0.1 is employed [18].

### 4.2. Comparisons with state-of-the-arts

According to the detailed experimental results in Tab. 4, the DeepGaitV2 and SwinGait series significantly outperform other state-of-the-art methods on OUMVLP [38], Gait3D [45], and GREW [46]. On the small-scale indoor dataset CASIA-B [44], however, all the proposed deep models exhibit no superiority, and the reasons for this have been thoroughly explained in Sec. 3.3. Notably, on the recently published in-the-wild datasets, *i.e.*, Gait3D and GREW, both DeepGaitV2-3D and SwinGait-3D have achieved remarkable performance improvements (about +30% on rank-1 accuracy on the challenging outdoor GREW). We hope the empirical principles outlined in Sec. 3 can provide guidance for further gait research.

Table 4. Comparison to state-of-the-art on CASIA-B [44], OU-MVLP [38], Gait3D [45] and GREW [46]. On the CASIA-B and OU-MVLP, the identical-view cases are excluded. The accuracy on CASIA-B is the average of three testing subsets.

Method	Source	Testing Datasets							
		CASIA-B [44]	OU-MVLP [38]	Gait3D [45]			GREW [46]		
		R-1 (%)	R-1 (%)	R-1 (%)	R-5 (%)	mAP (%)	R-1 (%)	R-5 (%)	R-10 (%)
GaitSet [4]	AAAI 2019	87.1	87.1	36.7	58.3	30.0	46.3	63.6	70.3
GaitPart [9]	CVPR 2022	88.5	88.7	28.2	47.6	21.6	44.0	60.7	67.3
GaitGL [24]	ICCV 2021	91.9	89.7	29.7	48.5	22.3	47.3	-	-
CSTL [19]	ICCV 2021	<b>93.5</b>	90.2	11.7	19.2	5.6	50.6	65.9	71.9
SMPLGait [45]	CVPR 2022	-	-	46.3	64.5	37.2	-	-	-

Proposed	#param.	FLOPs	CNN-based DeepGaitV2 series v.s. Transformer-based SwinGait series							
DeepGaitV2-2D	9.3M	2.4G	88.8	90.0	68.2	48.6	60.4	68.6	82.0	86.1
SwinGait-2D	10.9M	2.5G	-	-	69.4	84.6	61.6	70.8	83.7	87.6
DeepGaitV2-3D	27.5M	6.8G	89.6	<b>92.0</b>	72.8	86.2	63.9	<b>79.4</b>	<b>88.9</b>	91.4
DeepGaitV2-P3D	11.1M	2.9G	89.6	91.9	74.4	<b>88.0</b>	65.8	77.7	87.9	90.6
SwinGait-3D	13.1M	4.0G	-	-	<b>75.0</b>	86.7	<b>67.2</b>	79.3	<b>88.9</b>	<b>91.8</b>

Table 5. Ablation study of DeepGaitV2 and SwinGait series on Gait3D and GREW. The  $C$  and  $B$  respectively denote the arbitrary channel number and the block numbers accordingly shown in Tab. 1 and Figure 7.

Method	Control Condition	Gait3D R-1 (%)	GREW R-1 (%)	#param.	FLOPs
DeepGaitV2 -2D	$C=32$	62.9	62.2	2.3M	0.6G
	$C=64$	68.2	68.6	9.3M	2.4G
	$C=128$	69.5	71.8	37.3M	9.7G
DeepGaitV2 -3D	$C=32$	69.4	73.1	6.9M	1.7G
	$C=64$	72.8	79.4	27.5M	6.8G
	$C=128$	<b>75.8</b>	<b>81.6</b>	109.8M	27.2G
DeepGaitV2 -P3D	$C=32$	67.9	72.8	2.8M	0.7G
	$C=64$	74.4	77.7	11.1M	2.9G
	$C=128$	75.0	81.0	44.4M	11.4G
SwinGait -2D	$B=[1,2,2,2]$	68.7	67.4	8.8M	1.8G
	$B=[1,4,4,2]$	69.4	70.8	10.9M	2.46G
SwinGait -3D	$B=[1,2,2,2]$	69.0	77.3	9.8 M	2.5G
	$B=[1,4,4,2]$	75.0	79.3	13.1M	4.0G

### 4.3. DeepGaitV2 v.s. SwinGait

As shown in Tab. 4, the SwinGait series surpasses the corresponding CNN-based DeepGaitV2 model for most outdoor cases, considering the speed-accuracy trade-off. In our view, the evolution of network architectures is always worth keeping a close eye on, and Transformer is particularly noteworthy and popular for its use of attention to model both long-term and short-term dependencies. Since gait recognition relies on fine-grained spatiotemporal features, we hope the SwinGait series can contribute to the modeling shift from CNN to Transformer for further gait recognition research and applications.

### 4.4. Ablation study

The controlling settings directly determining the backbone capacity have been considered, *i.e.*, the network depth

and width. For the DeepGaitV2 series, Sec. 3.3 has exhibited the effectiveness of increasing network depth. Consequently, we suggest the 22-layer DeepGaitV2 as the baseline for outdoor gait datasets. Here, we further widen the DeepGaitV2 series, *i.e.*, enlarging  $C$  from 32 to 128 as shown in Tab. 5. Results show that the accuracy improves steadily, but the model size and computation cost increase dramatically. To cut the carbon emissions, we suggest the DeepGaitV2-P3D with  $C=64$  as the baseline model for the DeepGaitV2 series for a good balance. As for the SwinGait series, Tab. 5 shows that reasonably deepening the backbone can also bring performance gain.

## 5. Discussion and Future Work

The comprehensive study in the paper explores classical CNN-based and emerging Transformer-based architectures, covering three fundamental topics: suitable network capacity, explicit temporal modeling, and deep gait transformer for fine-grained gait description. Apart from achieving impressive performance breakthroughs on outdoor datasets, this study summarizes critical empirical principles for deep gait model construction from a unified perspective, based on extensive experimental analysis and discussion.

The study also reveals that, similar to many other vision tasks, increasing the depth and size of deep gait models is necessary when training on large gait datasets, even though the binary silhouette is considered structurally simple and characteristically sparse. Although the performance on the largest outdoor gait dataset, GREW [46], is impressive with a rank-1 accuracy of 81.6%, there is still a big gap to achieve a high enough gait recognition accuracy for real applications. Additionally, collecting and labeling gait video data is more expensive and difficult than most other vision tasks, making it a major challenge for improving gait recognition in the future. Feasible solutions are expected.

## References

- [1] Zhe Cao, Tomas Simon, Shih-En Wei, and Yaser Sheikh. Realtime multi-person 2d pose estimation using part affinity fields. In *Proceedings of the IEEE conference on computer vision and pattern recognition*, pages 7291–7299, 2017. [1](#)
- [2] Zhe Cao, Tomas Simon, Shih-En Wei, and Yaser Sheikh. Realtime multi-person 2d pose estimation using part affinity fields. In *Proceedings of the IEEE conference on computer vision and pattern recognition*, pages 7291–7299, 2017. [2](#)
- [3] Nicolas Carion, Francisco Massa, Gabriel Synnaeve, Nicolas Usunier, Alexander Kirillov, and Sergey Zagoruyko. End-to-end object detection with transformers. In *Computer Vision–ECCV 2020: 16th European Conference, Glasgow, UK, August 23–28, 2020, Proceedings, Part I 16*, pages 213–229. Springer, 2020. [7](#)
- [4] Hanqing Chao, Yiwei He, Junping Zhang, and Jianfeng Feng. Gaitset: Regarding gait as a set for cross-view gait recognition. In *Proceedings of the AAAI conference on artificial intelligence*, volume 33, pages 8126–8133, 2019. [1](#), [2](#), [3](#), [4](#), [5](#), [8](#)
- [5] Yufeng Cui and Yimei Kang. Gaittransformer: Multiple-temporal-scale transformer for cross-view gait recognition. In *2022 IEEE International Conference on Multimedia and Expo (ICME)*, pages 1–6, 2022. [3](#)
- [6] Alexey Dosovitskiy, Lucas Beyer, Alexander Kolesnikov, Dirk Weissenborn, Xiaohua Zhai, Thomas Unterthiner, Mostafa Dehghani, Matthias Minderer, Georg Heigold, Sylvain Gelly, et al. An image is worth 16x16 words: Transformers for image recognition at scale. *arXiv preprint arXiv:2010.11929*, 2020. [2](#), [3](#), [6](#)
- [7] Huanzhang Dou, Pengyi Zhang, Wei Su, Yunlong Yu, and Xi Li. Metagait: Learning to learn an omni sample adaptive representation for gait recognition. In *European Conference on Computer Vision*, pages 357–374. Springer, 2022. [2](#), [4](#)
- [8] Chao Fan, Junhao Liang, Chuanfu Shen, Saihui Hou, Yongzhen Huang, and Shiqi Yu. OpenGait: Revisiting gait recognition toward better practicality. *arXiv preprint arXiv:2211.06597*, 2022. [1](#), [2](#), [3](#), [7](#)
- [9] Chao Fan, Yunjie Peng, Chunshui Cao, Xu Liu, Saihui Hou, Jiannan Chi, Yongzhen Huang, Qing Li, and Zhiqiang He. Gaitpart: Temporal part-based model for gait recognition. In *Proceedings of the IEEE/CVF conference on computer vision and pattern recognition*, pages 14225–14233, 2020. [2](#), [3](#), [4](#), [8](#)
- [10] Yang Fu, Yunchao Wei, Yuqian Zhou, Honghui Shi, Gao Huang, Xinchao Wang, Zhiqiang Yao, and Thomas Huang. Horizontal pyramid matching for person re-identification. In *Proceedings of the AAAI conference on artificial intelligence*, volume 33, pages 8295–8302, 2019. [3](#)
- [11] Xinqian Gu, Hong Chang, Bingpeng Ma, Shutao Bai, Shiguang Shan, and Xilin Chen. Clothes-changing person re-identification with rgb modality only. In *Proceedings of the IEEE/CVF Conference on Computer Vision and Pattern Recognition*, pages 1060–1069, 2022. [2](#), [3](#), [5](#)
- [12] Kensho Hara, Hirokatsu Kataoka, and Yutaka Satoh. Learning spatio-temporal features with 3d residual networks for action recognition. In *Proceedings of the IEEE international conference on computer vision workshops*, pages 3154–3160, 2017. [3](#)
- [13] Kaiming He, Xiangyu Zhang, Shaoqing Ren, and Jian Sun. Deep residual learning for image recognition. In *Proceedings of the IEEE Conference on Computer Vision and Pattern Recognition*, pages 770–778, 2016. [1](#), [3](#), [4](#), [5](#)
- [14] Alexander Hermans, Lucas Beyer, and Bastian Leibe. In defense of the triplet loss for person re-identification. *arXiv preprint arXiv:1703.07737*, 2017. [7](#)
- [15] Saihui Hou, Chunshui Cao, Xu Liu, and Yongzhen Huang. Gait lateral network: Learning discriminative and compact representations for gait recognition. In *European conference on computer vision*, pages 382–398. Springer, 2020. [2](#)
- [16] Saihui Hou, Xu Liu, Chunshui Cao, and Yongzhen Huang. Set residual network for silhouette-based gait recognition. *IEEE Transactions on Biometrics, Behavior, and Identity Science*, 3(3):384–393, 2021. [2](#), [5](#)
- [17] Gao Huang, Zhuang Liu, Laurens Van Der Maaten, and Kilian Q Weinberger. Densely connected convolutional networks. In *Proceedings of the IEEE conference on computer vision and pattern recognition*, pages 4700–4708, 2017. [4](#)
- [18] Gao Huang, Yu Sun, Zhuang Liu, Daniel Sedra, and Kilian Q Weinberger. Deep networks with stochastic depth. In *Computer Vision–ECCV 2016: 14th European Conference, Amsterdam, The Netherlands, October 11–14, 2016, Proceedings, Part IV 14*, pages 646–661. Springer, 2016. [7](#)
- [19] Xiaohu Huang, Duowang Zhu, Hao Wang, Xinggong Wang, Bo Yang, Botao He, Wenyu Liu, and Bin Feng. Context-sensitive temporal feature learning for gait recognition. In *Proceedings of the IEEE/CVF International Conference on Computer Vision*, pages 12909–12918, 2021. [4](#), [8](#)
- [20] Xin Jin, Tianyu He, Kecheng Zheng, Zhiheng Yin, Xu Shen, Zhen Huang, Ruoyu Feng, Jianqiang Huang, Zhibo Chen, and Xian-Sheng Hua. Cloth-changing person re-identification from a single image with gait prediction and regularization. In *Proceedings of the IEEE/CVF Conference on Computer Vision and Pattern Recognition*, pages 14278–14287, 2022. [2](#), [3](#), [5](#)
- [21] Alex Krizhevsky, Ilya Sutskever, and Geoffrey E Hinton. Imagenet classification with deep convolutional neural networks. In F. Pereira, C.J. Burges, L. Bottou, and K.Q. Weinberger, editors, *Advances in Neural Information Processing Systems*, volume 25. Curran Associates, Inc., 2012. [4](#)
- [22] Xiang Li, Yasushi Makihara, Chi Xu, Yasushi Yagi, Shiqi Yu, and Mingwu Ren. End-to-end model-based gait recognition. In *Proceedings of the Asian conference on computer vision*, 2020. [2](#)
- [23] Rijun Liao, Shiqi Yu, Weizhi An, and Yongzhen Huang. A model-based gait recognition method with body pose and human prior knowledge. *Pattern Recognition*, 98:107069, 2020. [2](#)
- [24] Beibei Lin, Shunli Zhang, and Xin Yu. Gait recognition via effective global-local feature representation and local temporal aggregation. In *Proceedings of the IEEE/CVF International Conference on Computer Vision*, pages 14648–14656, 2021. [2](#), [3](#), [4](#), [8](#)
- [25] Ze Liu, Yutong Lin, Yue Cao, Han Hu, Yixuan Wei, Zheng Zhang, Stephen Lin, and Baining Guo. Swin transformer:

- Hierarchical vision transformer using shifted windows. In *Proceedings of the IEEE/CVF International Conference on Computer Vision*, pages 10012–10022, 2021. 2, 3, 6, 7
- [26] Ze Liu, Jia Ning, Yue Cao, Yixuan Wei, Zheng Zhang, Stephen Lin, and Han Hu. Video swin transformer. In *Proceedings of the IEEE/CVF Conference on Computer Vision and Pattern Recognition*, pages 3202–3211, 2022. 3, 6, 7
- [27] Jonathan Long, Evan Shelhamer, and Trevor Darrell. Fully convolutional networks for semantic segmentation. In *Proceedings of the IEEE conference on computer vision and pattern recognition*, pages 3431–3440, 2015. 1
- [28] Matthew Loper, Naureen Mahmood, Javier Romero, Gerard Pons-Moll, and Michael J Black. Smpl: A skinned multi-person linear model. *ACM transactions on graphics (TOG)*, 34(6):1–16, 2015. 2
- [29] Ilya Loshchilov and Frank Hutter. Fixing weight decay regularization in adam. arxiv 2017. *arXiv preprint arXiv:1711.05101*, 2017. 7
- [30] Hao Luo, Youzhi Gu, Xingyu Liao, Shenqi Lai, and Wei Jiang. Bag of tricks and a strong baseline for deep person re-identification. In *Proceedings of the IEEE/CVF conference on computer vision and pattern recognition workshops*, pages 0–0, 2019. 3, 4
- [31] Julieta Martinez, Rayat Hossain, Javier Romero, and James J Little. A simple yet effective baseline for 3d human pose estimation. In *Proceedings of the IEEE international conference on computer vision*, pages 2640–2649, 2017. 2
- [32] Jashila Nair Mogan, Chin Poo Lee, Kian Ming Lim, and Kalaiarasi Sonai Muthu. Gait-vit: Gait recognition with vision transformer. *Sensors*, 22(19):7362, 2022. 3
- [33] Mark S Nixon and John N Carter. Automatic recognition by gait. *Proceedings of the IEEE*, 94(11):2013–2024, 2006. 1
- [34] Domagoj Pinčić, Diego Sušan, and Kristijan Lenac. Gait recognition with self-supervised learning of gait features based on vision transformers. *Sensors*, 22(19):7140, 2022. 3
- [35] Zhaofan Qiu, Ting Yao, and Tao Mei. Learning spatio-temporal representation with pseudo-3d residual networks. In *proceedings of the IEEE International Conference on Computer Vision*, pages 5533–5541, 2017. 3, 5
- [36] Shaoqing Ren, Kaiming He, Ross Girshick, and Jian Sun. Faster r-cnn: Towards real-time object detection with region proposal networks. *Advances in neural information processing systems*, 28, 2015. 1
- [37] Yifan Sun, Liang Zheng, Yi Yang, Qi Tian, and Shengjin Wang. Beyond part models: Person retrieval with refined part pooling (and a strong convolutional baseline). In *Proceedings of the European conference on computer vision (ECCV)*, pages 480–496, 2018. 3
- [38] Noriko Takemura, Yasushi Makihara, Daigo Muramatsu, Tomio Echigo, and Yasushi Yagi. Multi-view large population gait dataset and its performance evaluation for cross-view gait recognition. *IPSJ Transactions on Computer Vision and Applications*, 10(1):1–14, 2018. 1, 2, 4, 5, 7, 8
- [39] Ashish Vaswani, Noam Shazeer, Niki Parmar, Jakob Uszkoreit, Llion Jones, Aidan N Gomez, Łukasz Kaiser, and Illia Polosukhin. Attention is all you need. *Advances in neural information processing systems*, 30, 2017. 2, 6
- [40] Limin Wang, Yuanjun Xiong, Zhe Wang, Yu Qiao, Dahua Lin, Xiaoou Tang, and Luc Van Gool. Temporal segment networks: Towards good practices for deep action recognition. In *European conference on computer vision*, pages 20–36. Springer, 2016. 1
- [41] Thomas Wolf, Mohammadreza Babae, and Gerhard Rigoll. Multi-view gait recognition using 3d convolutional neural networks. In *2016 IEEE international conference on image processing (ICIP)*, pages 4165–4169. IEEE, 2016. 2
- [42] Zifeng Wu, Yongzhen Huang, Liang Wang, Xiaogang Wang, and Tieniu Tan. A comprehensive study on cross-view gait based human identification with deep cnns. *IEEE transactions on pattern analysis and machine intelligence*, 39(2):209–226, 2016. 1, 2
- [43] Chi Xu, Yasushi Makihara, Xiang Li, Yasushi Yagi, and Jianfeng Lu. Gait recognition from a single image using a phase-aware gait cycle reconstruction network. In *European Conference on Computer Vision*, pages 386–403. Springer, 2020. 5
- [44] Shiqi Yu, Daoliang Tan, and Tieniu Tan. A framework for evaluating the effect of view angle, clothing and carrying condition on gait recognition. In *18th International Conference on Pattern Recognition (ICPR'06)*, volume 4, pages 441–444. IEEE, 2006. 1, 2, 4, 5, 7, 8
- [45] Jinkai Zheng, Xinchun Liu, Wu Liu, Lingxiao He, Chenggang Yan, and Tao Mei. Gait recognition in the wild with dense 3d representations and a benchmark. In *Proceedings of the IEEE/CVF Conference on Computer Vision and Pattern Recognition*, pages 20228–20237, 2022. 1, 2, 3, 4, 5, 6, 7, 8
- [46] Zheng Zhu, Xianda Guo, Tian Yang, Junjie Huang, Jiankang Deng, Guan Huang, Dalong Du, Jiwen Lu, and Jie Zhou. Gait recognition in the wild: A benchmark. In *Proceedings of the IEEE/CVF international conference on computer vision*, pages 14789–14799, 2021. 1, 2, 3, 4, 5, 6, 7, 8